CFD Modeling using STAR-CCM+ Commercial Code of Liquid Mixing and Stratification in a Simulated Protected Loss of Power Transient in the Gallium Thermal-hydraulic Experiment (GaTE)

Mohamed S. El-Genk, Timothy M. Schriener, Keenan Kresl-Hotz
Institute for Space and Nuclear Power Studies and NE Department
The University of New Mexico, Albuquerque, NM

UNM-ISNPS Technical Report ISNPS-03-2025

Second Year Annual Report

Supported by a Department of Energy Nuclear Engineering University Program Integrated Research Project grant DE-NE0009420 through a subaward from the City College of New York to the University of New Mexico CM00011961-00.

October 2025

CFD Modeling of Liquid Mixing and Stratification during a Simulated Protected Loss of Power Transient in the Gallium Thermal-hydraulic Experiment (GaTE) using STAR-CCM+

Mohamed S. El-Genk, Timothy M. Schriener, Keenan Kresl-Hotz
Institute for Space and Nuclear Power Studies and NE Department
The University of New Mexico, Albuquerque, NM

Abstract

This report details the progress made at the University of New Mexico's Institute for Space and Nuclear Power Studies (UNM-ISNPS) during the second year of an Integrated Research Project (IRP) led by City College of New York (CCNY) and entitled: *Exascale Simulation of Thermal-Hydraulics Phenomena in Advanced Reactors and Validation Using High Resolution Experimental Data*. The objective is to develop research capabilities in large scale Computational Fluid Dynamics (CFD) modeling and simulation and apply them to simulate thermal-hydraulics phenomena in advanced reactors and benchmark the results of these simulations against scaled experiments. The performed CFD analyses at the UNM-ISNPS as part of this award are of the Protected Loss of Power (PLOP) experiments conducted using the Gallium Thermal-hydraulic Experiment (GaTE) facility at Purdue University. The experiment investigated thermal stratification phenomena of liquid gallium akin to that in the upper plenum of pool-type sodium fast reactors. The performed CFD analyses using the STAR-CCM+ commercial Multiphysics code are of liquid Ga mixing and stratification in the upper plenum of the test vessel in the experiment

In addition to investigating the formation of the liquid mixing eddies, the present analyses calculate the temperature and average velocity distributions in the plenum and compare the results for a rigid and a non-rigid liquid gallium free surface. The performed CFD analyses used the Large Eddy Simulation (LES) turbulence model to predict the complex liquid mixing patterns which could not adequately be resolved using the (Unsteady Reynolds Average Navier Stokes) URANS SST k-ω turbulence model. Results also show that the thickness of the hot liquid stratified layer near the free surface in the upper plenum progressively decreases with increasing the injection rate of the cooler liquid gallium into the plenum and the time of the simulated transients. With a non-rigid gallium free surface, extensive formation of small turbulent mixing eddies occurs in the top section of the plenum and the thickness of the hot liquid stratified layer decreases slightly faster with time than with a rigid free surface. Simulation results of the axial distributions of the liquid temperature and the time averaged flow velocity in the plenum are in good agreement with reported measurements in the PLOP40 and PLOP60 experiments for injection rates of the cooler gallium into the upper plenum of 0.524 and 0.786 kg/s, respectively.

Nomenclature

ABTR	Advanced Burner Test Reactor
ANL	Argonne National Laboratory
CFD	Computational Fluid Dynamics
DES	Detached Eddy Simulation
DNS	Direct Numerical Simulation
DTS	Distributed Temperature System
GaTE	Gallium Thermal-hydraulic Experiment
GCI	Grid Conversion Index
HEX	Heat exchanger
HRIC	High-Resolution Interface Capturing
IMD	Interface Momentum Dissipation
k	Turbulent kinetic energy (J/kg)
k_{res}	Turbulent kinetic energy for the resolved or filtered turbulence
k_{sgs}	Turbulent kinetic energy of the residual turbulence in the flow (J/kg)
LBE	Lead Bismuth Eutectic
LES	Large Eddy Simulation
N	Number of numerical mesh cells
PLOF	Protected Loss of Flow
PLOH-LOF	Protected Loss of Heat Sink and Loss of Flow
PLOP	Protected Loss of Power
r	Radial coordinate (m)
r_n	Numerical mesh refinement ratio
R	Calculated fraction of the total turbulent kinetic energy by subgrid scale model
RANS	Reynolds Averaged Navier Stokes
SFR	Sodium Fast Reactor
SST	Sheer Stress Transport
T	Temperature (K)
T_o	Isothermal pre-test gallium temperature (K)
T_{TC}	Measured gallium inlet temperature (K)
TC	Thermocouple
UDV	Ultrasonic Doppler Velocimeter

UIS	Upper Instrumentation Structure
UNM-ISNPS	University of New Mexico's Institute for Space and Nuclear Power Studies
URANS	Unsteady Reynolds Averaged Navier Stokes
VOF	Volume of Fluid
WALE	Wall-Adapting Local Eddy-viscosity
Z	Axial distance from bottom of the upper plenum (m)

Greeks

ε	Relative error
ρ	Order of the numerical method

1.0 Introduction

Advanced pool-type Sodium Fast Reactors (SFRs) offer significant operation, performance, and safety advantages. They operate at high temperatures for thermo-chemical production of hydrogen and other industrial applications and high plant thermal efficiency. Their operation slightly below atmospheric pressure owing to the low vapor pressure of liquid sodium (Na) eliminates the need for a heavy pressure vessel and provides a large temperature margin from the boiling point. The high operating temperature of these reactors is compatible with using a superheated steam Rankine cycle (Fig. 1) or supercritical CO_2 closed Brayton cycle for energy conversion [US DOE 2021; IAEA 2013]. The submerged intermediate Na-Na heat exchanger (HEX) in the Na hot pool or plenum enhances safety, and the large inventory of liquid Na in the pool provides a large thermal mass for the passive storage of decay heat after reactor shutdown (Fig. 1).

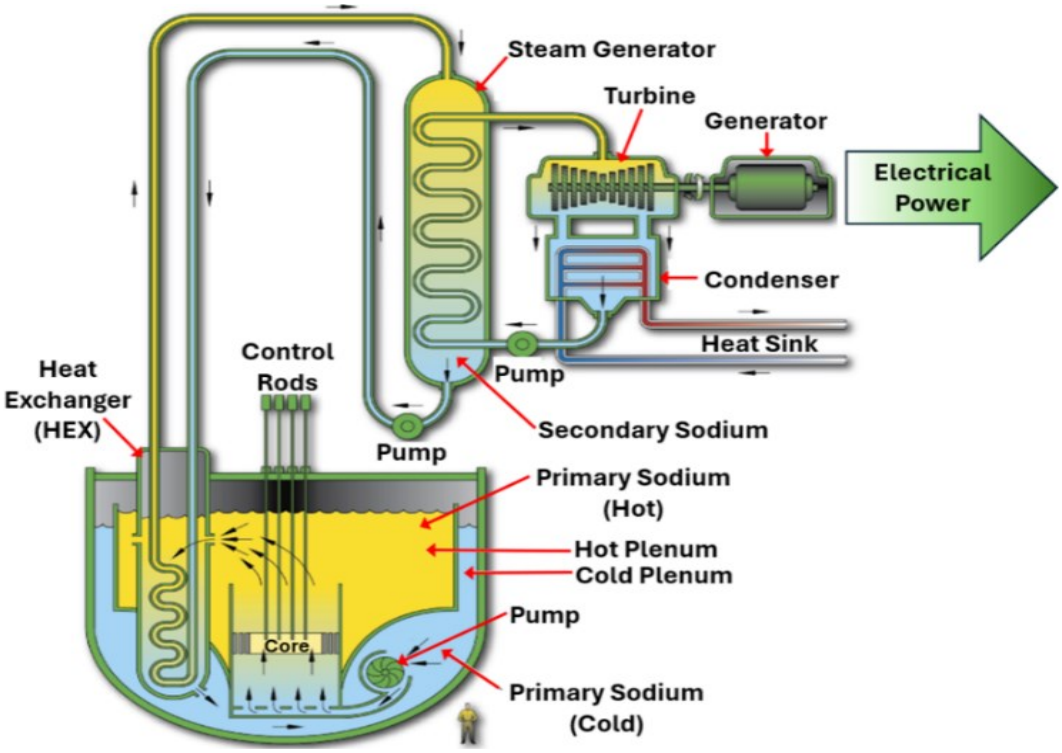

Fig. 1. Layout of a representative Gen-IV pool-type sodium fast reactor [US DOE 2021].

During nominal operation, the temperature of liquid Na in the upper plenum of the SFR pool is close to that of the Na exiting the reactor core. Following a sudden decrease in reactor power or a scram, the temperature of the liquid sodium that exits the core decreases below nominal. This cooler Na mixes with the hot Na in the upper plenum above the core and a stratified layer of hot Na forms below the pool free surface and above the intake of the Na-Na HEX (Fig. 1). In a postulated Protected Loss of Power (PLOP) event the submerged primary pump in the Na pool continues to circulate the coolant through the reactor core. The liquid mixing and the oscillation of the thermal stratified layer in the upper plenum can induce thermal stress in the metallic components of the reactor core [Wu, et al. 2020]. Such components include the Upper Instrumentation Structure (UIS) above the core that contains the control element drives and in-core instrumentation tubes (Fig. 1), the reactor vessel, the outer shell of the submerged Na-Na HEX, and the upper section of the reactor core. The resulting thermal fatigue cracking due to cyclic stresses may fail or damage these components.

To assess the consequences and quantify potential effects of a postulated PLOP event in pool-type SFRs researchers have performed small scale simulation experiments and conducted transient numerical Computational Fluid Dynamics (CFD) analyses. In these analyses simulating the thermal stratification in pool-type SFRs has proved to be challenging. Some reported significant differences between the analyses predictions and reported measurements for 1/10 and 1/20 scale experiments and small test loops [Ohno, et al. 2011; Mochizuki and Yao 2014; Sakamoto, et al. 2010; Hu, et al. 2013; Zwijsen, et al. 2019; Ward, Hopkins, and Bindra 2020]. Recently, Ward, Clark, and Bindra [2019] constructed the Gallium Thermal-hydraulic Experiment (GaTE) to simulate liquid flow mixing and thermal stratification in the upper pool of SFRs (Fig. 2). The GaTE facility is a 1/20 scale of the upper plenum of the US DOE Advanced Burner Test Reactor (ABTR) concept [Chang, Frinck and Grandy 2008] and comprises a flow loop for circulating low melting point liquid gallium (Ga) using a moving magnet pump (Fig. 2). The liquid gallium in the loop is heated before entering the upper plenum in the experiments using a tube-in-shell oil circulation heat exchanger and cooled after exiting the plenum using two tube-in-shell water HEXs connected to the horizontal outlet legs [Ward, Clark, and Bindra 2019] (Figs. 1-3).

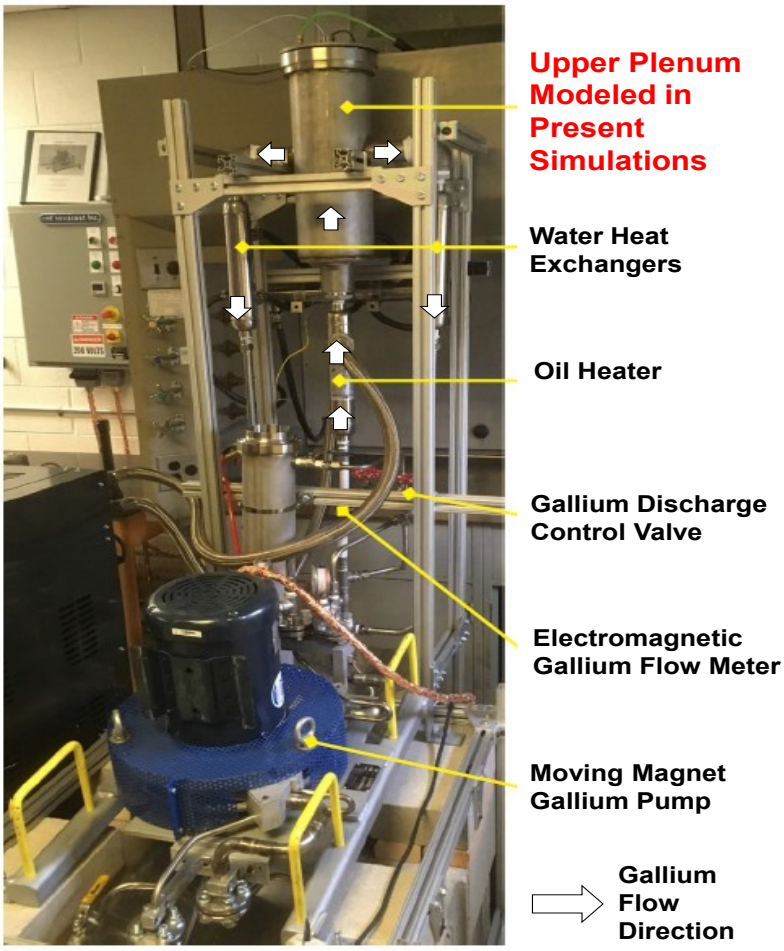

Fig. 2. Gallium Thermal-hydraulic Facility [modified from Ward, Clark, and Bindra 2019].

The experiments performed in the GaTE facility simulated PLOP events in pool type SFRs by tripping the heater at the start of the transient to decrease the temperature of the liquid gallium entering the upper plenum by 50 K, from an initial value of 373.15 K to 323.15 K, while maintaining a constant flow rate [Ward, Clark, and Bindra 2019]. The PLOP experiments were performed at uniform inlet velocities of the cooler liquid gallium into the upper plenum, ranging from 2.39 to 80 mm/s, for corresponding inlet

Reynolds numbers of 422 – 1.41×10^4 [Ward, Clark, and Bindra 2019]. They measured the local temperatures and velocities of liquid gallium and reported the flow mixing during the performed PLOP transients. The performed CFD analyses of the GaTE experiments using the Fluent commercial CFD code [Ward, Hopkins, and Bindra 2020; Bindra, et al. 2020] employed a LES turbulence model with the wall-adapting local eddy-viscosity (WALE) subgrid scale model. The analyses simplified the shape of the inlet and outlet ducts, didn't include the internal instrumentation rack structure, and assumed a rigid liquid gallium free surface (Fig. 3). They did not report mesh grid refinement analyses, however, the calculated time-averaged velocities in the upper plenum were in good agreement with the experimental measurements using an Ultrasonic Doppler Velocimeter (UDV) sensor (Fig. 2).
For simplicity, reported CFD analyses of simulating liquid mixing and stratification in upper plenum of pool-type SFRs mostly utilized RANS turbulence models and assumed a rigid liquid free surface [Mochizuki and Yao 2014; Sakamoto, et al. 2010; Zwijsen, et al. 2019; Ward, Hopkins, and Bindra 2020; Bindra, et al. 2020]. A few have used a multi-component Volume of Fluid (VOF) model to simulate a non-rigid free surface in the upper plenum but did not report the impact on the CFD results [Hu, et al. 2013]. None have investigated the effects on the simulation results of using the more advanced LES turbulence models instead of the simpler RANS turbulence models. The k-ε and k-ω, two-equations RANS turbulence models use approximations to solve the Reynolds stresses in the flow [Launder and Spalding 1974], while the LES turbulence models directly resolve the turbulence of larger eddies and captures flow eddies with length scales smaller than the specified filter scale using a subgrid-scale model [Smagorinsky 1963]. Thus, the LES models have been used successfully to simulate complex turbulent behavior, such as those in swirling and jetting flows, more accurately than the RANS models [Larocque 2004; Rodriguez and El-Genk 2011] but at higher computational cost [Siemens PLM 2023].

During the 2nd year of the 2023 DOE NUEP IRP *Exascale Simulation of Thermal-Hydraulics Phenomena in Advanced Reactors and Validation Using High Resolution Experimental Data*, the University of New Mexico's Institute for Space and Nuclear Power Studies (UNM-ISNPS) focused on the benchmarking analyses in Tasks 2 and 3 of the CFD simulations of the Protected Loss of Power (PLOP) experiments conducted using the Gallium Thermal-hydraulic Experiment (GaTE) facility at Purdue University. The objectives of this work are to (a) conduct CFD analyses to simulate flow mixing and stratification of hot liquid gallium below the free surface in the upper plenum of the PLOP experiments performed at the GaTE facility [Ward, Clark, and Bindra 2019], (b) investigate the effects on the CFD results of refining the numerical mesh grid, the choice of the turbulence model, and employing a rigid and a non-rigid liquid free surface, and (c) benchmark the results of the CFD simulations with the reported experimental measurements. The performed CFD analyses use the STAR-CCM+ commercial code [Siemens PLM 2023] and investigate both the LES and RANS SST k-ω turbulence models to simulate flow mixing of liquid gallium in the GaTE upper plenum. Transient simulations are performed of the PLOP40 and PLOP60 experiments [Ward, Clark, and Bindra 2019] with liquid gallium inlet flow rates of 0.524 and 0.786 kg/s. The results quantify the effects of employing a rigid and a non-rigid liquid free surface on the gallium flow mixing and the time-dependent axial distributions of the local temperature and the time averaged flow velocities. The CFD results are then compared to the reported measurements in the experiments and the CFD results of Bindra et al. [Bindra, et al. 2020].

2.0 GaTE Facility at Purdue University

The integrated GaTE facility at Purdue University (Fig. 2) is a 1/20th scale representation of the ABTR [Ward, Clark, and Bindra 2019], a 250 MW_{th}, pool-type SFR concept developed at Argonne National Laboratory (ANL) to demonstrate transmutation of transuranic waste [Chang, Frinck and Grandy 2008]. Fig. 3 shows two section views of the upper plenum of the GaTE facility for the PLOP experiments. The inlet at the bottom of the plenum represents the liquid metal flow that exits the reactor core into the upper plenum of the liquid sodium in the pool-type ABTR. The two horizontal discharge legs represent the

location of the inlet flow to the in-vessel HEX (Figs. 1, 3) [Ward, Clark, and Bindra 2019]. A moving magnet pump near the bottom of the GaTE facility loop circulates the molten gallium through upper plenum and an electromagnetic flowmeter measures the flow rate.

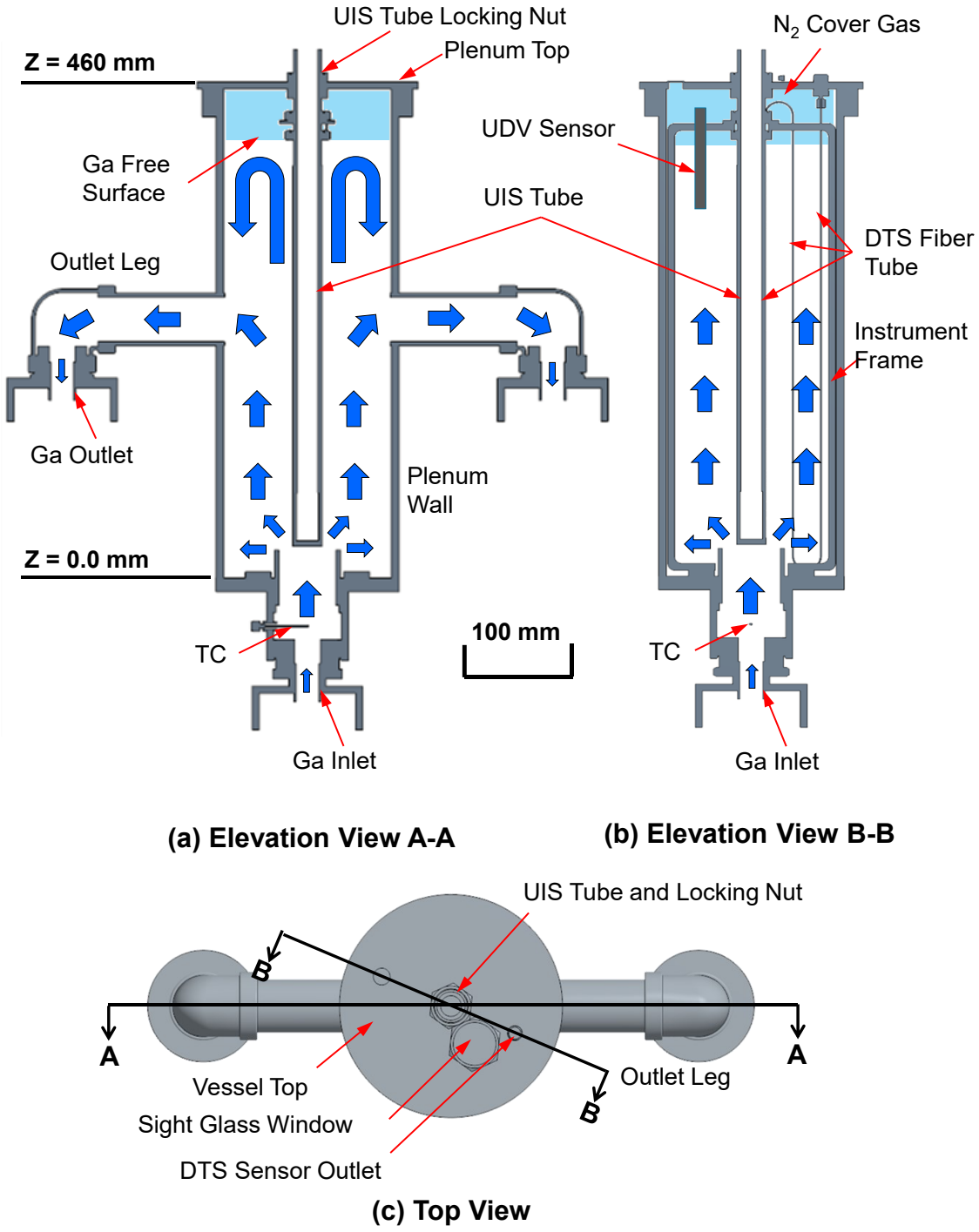

Fig. 3. Cutaway section views of the upper plenum in the GaTE facility.

The structure of GaTE facility is thermally insulated and the initial temperature of molten gallium in upper plenum is maintained constant at 373.15 K with the aid of a tube and shell mineral oil – gallium HEX (Fig. 2). A 1/16" diameter K-type thermocouple (TC) measures the liquid Ga temperature at the center of the inlet flow nozzle (Fig. 3) to within ± 0.75 °C [Ward, Clark, and Bindra 2019]. The cooler liquid gallium exits the mineral oil HEX and enters through the bottom of the upper plenum where it mixes with the residing gallium initially at 373.15 K in the upper plenum (Figs. 2 and 3). The liquid Ga in the plenum exits through two horizontal discharge legs on either side (Figs. 2 and 3). The liquid Ga free surface in the upper plenum is covered by a layer of inert nitrogen (N_2) gas at atmospheric pressure to minimize liquid surface oxidation (Fig. 3) like the argon cover gas in pool type SFRs (Fig. 1). The central stainless-steel tube in the plenum (Fig. 3) represents the UIS in an SFR. The liquid gallium that exits the horizontal legs flows through two tube and shell water HEXs for cooling (Figs. 2 and 3). These HEXs are analogous to the intermediate HEXs in a SFR hot pool (Fig. 1). The cooled liquid gallium returns to the pump to be circulated back into the plenum (Fig. 2).

The instruments in the GaTE test facility measure the spatial distributions of the local temperature and flow velocity of liquid gallium in the upper plenum. The liquid gallium temperatures within the upper plenum are measured using a Distributed Temperature Sensor (DTS) mounted to an internal rectangular frame (Fig. 3). The frame is rotated 23° from the plane that passes through the center of the two horizontal outlet legs (Section B-B in Fig. 3c). The DTS uses optical frequency domain reflectometry in two independent optical fiber tubes to measure the liquid temperatures. The stainless steel sheath enclosing the tubes is bent within the upper plenum to form three straight vertical sections at: (a) an 'inner' radial position, r = 11.75 mm from the center line and within a grove along the length of the UIS tube wall, (b) a 'middle' radial position r = 35.56 mm from the center line, and (c) an 'outer' radial position, r = 56.90 mm from the center line (Figs. 3a and b). The DTS Sensor measures the liquid gallium temperatures in the upper plenum within ± 1.8 °C and at frequencies up to 22.7 Hz [Ward, Clark, and Bindra 2019].

The UDV sensor mounted vertically opposite the DTS optical fiber (Fig. 3) measures the axial component of the gallium flow velocity, based on reflecting ultrasonic waves off gallium-oxide particles suspended within the liquid gallium in the upper plenum [Ward, Clark, and Bindra 2019]. The UDV sensor can be moved to different radial positions of r = 36, 47, and 58 mm from the center line (Fig. 3b). A second UDV sensor mounted inside the central UIS tube measures the velocity of the liquid gallium flow in the inlet tube above the TC location (Fig. 3a). The UDV sensors measure axial velocity at a frequency of 18.8 Hz and with uncertainty of ±2.5 mm/s [Ward, Clark, and Bindra 2019].

2.1 Protected Loss of Power (PLOP) Experiments

Prior to initiating the PLOP experiments in the GaTE facility, the circulating liquid gallium in the upper plenum is kept at constant temperature, T_o = 373.15, and a constant flow rate [Ward, Clark, and Bindra 2019]. The PLOP event is initiated by tripping the power to the mineral oil heater to decrease the temperature of the liquid gallium entering the upper plenum by 50 K, from 373.15 K to 323.15 K, with the circulation pump maintaining a specified inlet flow rate (Fig. 3). The cooler liquid gallium entering the upper plenum mixes with and displaces the hot gallium. Eventually a stratified layer of hot gallium forms below the free surface and above the location of the side outlet discharges [Ward, Clark, and Bindra 2019]. The experiments continue until the mean temperature of the liquid gallium exiting through the side discharge tubes reaches 323.15 K.

The performed CFD analyses of the transient PLOP experiments in the present work investigate the effect of changing the inlet flow rates of the cooler liquid gallium into the plenum from 0.375 to 2.246 kg/s on the induced liquid mixing and the formation of a Ga stratified layer in the GaTE upper plenum below the free surface. The reported CFD analyses by Ward, Hopkins, and Bindra [2020] modeled the performed

transitions to lower gallium inlet temperature in the experiments as step functions. They justified that because of the very short time between tripping the heater power and the actual decrease in the temperature of liquid gallium entering the upper plenum, from 373.15 to 323.15 K [Ward, Hopkins, and Bindra 2020]. The present CFD analyses investigate the effects on the results of modeling the decrease in the temperature of the liquid gallium entering the upper plenum at the beginning of the PLOP transient (time t = 0.0 s) both as a step function and using a time dependent fit of the reported inlet TC measurements in the experiments [Ward, Clark, and Bindra 2019]. These analyses also model the pre-test isothermal flow mixing of liquid gallium at 373.15 K in the upper plenum to establish the conditions prior to initiating the transients in the PLOP experiments.

3.0 CFD Methodology

The present analyses of the PLOP experiments are performed using the STAR-CCM+ commercial CFD code [Siemens PLM 2023] of the stainless-steel upper plenum (Fig. 3) and include the internal instrument frame with the DTS fiber tube in the upper plenum. Purdue University researchers provided the solid CAD geometry files of the GaTE facility. The files are simplified to smooth the helical threading on the pipes and hence decrease the number of numerical mesh cells employed and the computational cost without affecting the calculated results. The present CFD analyses apply the following boundary conditions: a constant gallium mass flow rate into the upper plenum and a constant pressure of the liquid gallium at the exit of the side discharge legs (Fig. 3). The insulated outer surface of the 316 stainless-steel upper plenum is modeled as an adiabatic boundary. The performed CFD analyses of the PLOP experiments investigated the effects of using the Sheer Stress Transport (SST) k-ω RANS turbulence model and the more sophisticated LES turbulence model on flow mixing and the liquid stratification in the upper plenum. These analyses are for both rigid and non-rigid liquid gallium free surfaces.

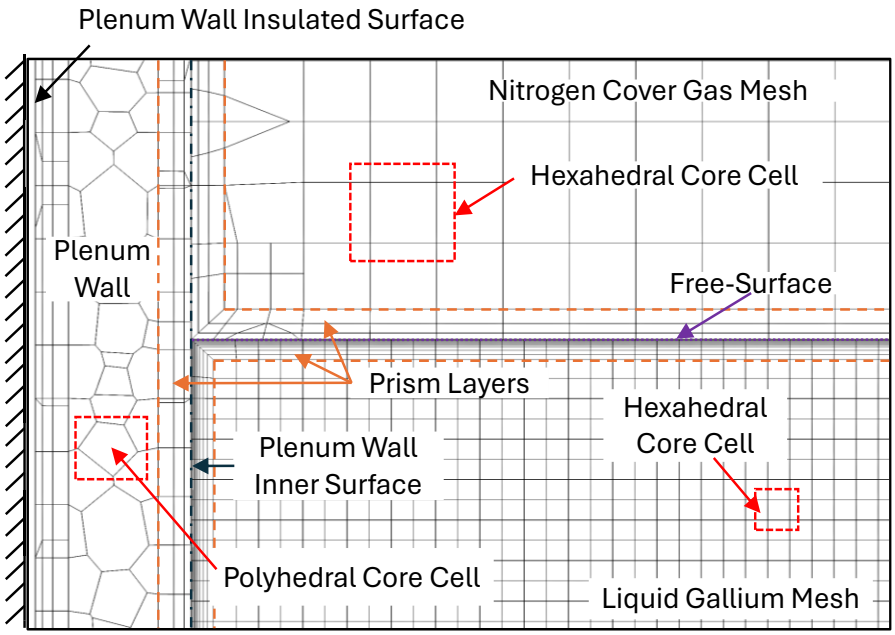

Fig. 4. Implemented numerical mesh grids in present CFD simulations with liquid Ga free surface in the upper plenums of the PLOP experiments conducted in the GaTE facility (Fig. 3a).

In the CFD analyses, the LES turbulence model in the CFD analyses calculates the turbulent kinetic energies for the eddies with length scales smaller than the filter size in the Wall-Adapting Local Eddy-viscosity (WALE) subgrid scale model, with the default input parameters [Siemens PLM 2023]. The CFD analyses of the PLOP experiments used both the LES and the Unsteady RANS (URANS) turbulence

models in the STAR-CCM+ code. They employed an implicit unsteady solver with a time step size of 0.01s and ten inner iterations per timestep and accounted for the changes in thermophysical properties of liquid gallium [Zamora 2020; Assael, et al. 2012] and N_2 cover gas [Lemmon, et al. 2024] with temperature.

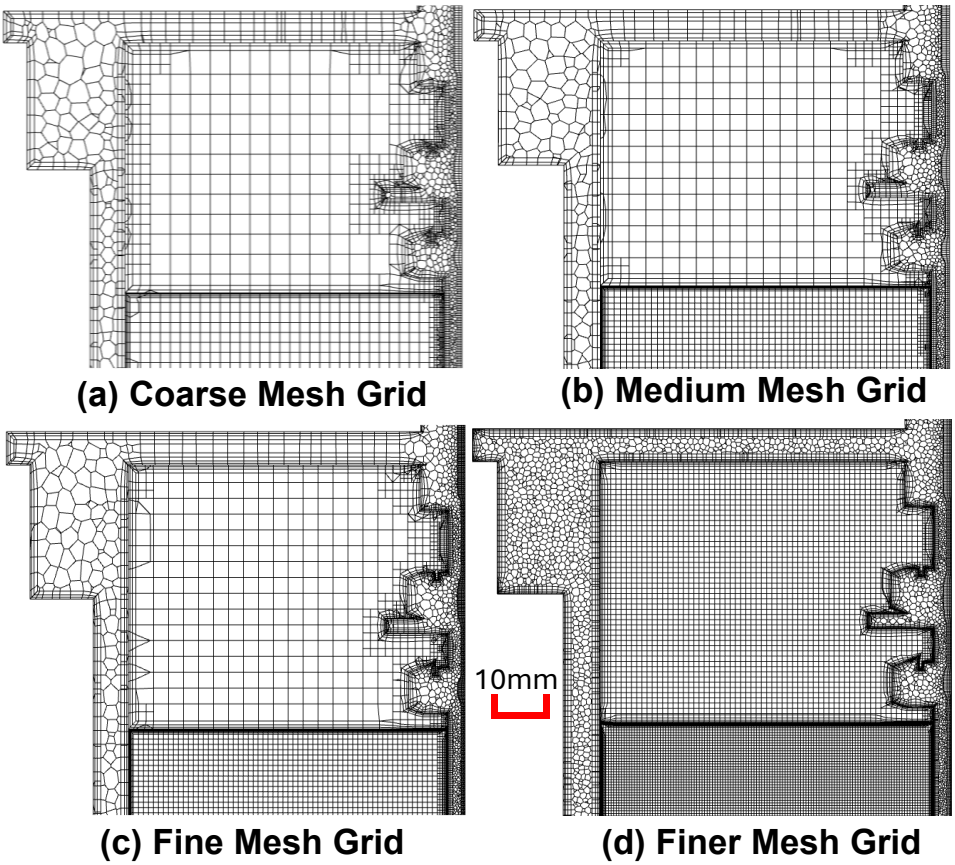

Fig. 5. Comparison of implemented numerical mesh grids (Coarse, Medium, Fine, and Finer) in present CFD analyses of liquid Ga in the upper plenum of PLOP experiments (Fig. 3a).

3.1 Treatment of Liquid gallium free surface in the upper plenum

In the CFD analyses of the PLOP experiments the liquid gallium free surface in the upper plenum is 0.0564 m below the top (Fig. 3c) and the space above the surface is filled with N_2 gas at atmospheric pressure. The present work investigated the liquid gallium flow mixing and the formation of a stratified layer in the upper plenum of the PLOP experiments and the effects of applying a rigid and a non-rigid free surface on the results. A rigid free surface simplifies the analyses as the liquid gallium below the surface is decoupled from the N_2 cover gas (Fig. 3). Conversely, the analysis with a non-rigid free surface couples the interaction of liquid gallium below the surface with the N_2 cover gas using the Volume of Fluid (VOF) model in the STAR-CCM+ code [Siemens PLM 2023]. The Eulerian tracking VOF model of the interface between immiscible phases has been used successfully to treat the free surface of hot sodium free surface in pool type SFRs [Hu, et al. 2013]. The implemented VOF model with High-Resolution Interface Capturing (HRIC) treats a sharp liquid-gas interface using a 2nd order face density reconstruction option with default angle factor of 0.05 [Siemens PLM 2023]. The interface momentum dissipation (IMD) model in the analysis uses an artificial interfacial viscosity of unity to prevent the formation of non-physical parasitic velocity currents within the VOF momentum balance of the free surface [Siemens PLM 2023].

3.2 Numerical mesh grid refinement

The present CFD analyses investigated the effects of refining the numerical mesh grid using the Trimmer meshing model in the STAR-CCM+ code [Siemens PLM 2023] on the liquid gallium mixing and stratification in the upper plenum, the solution convergence, and the computation time. The meshing model generates regular hexahedral mesh elements in the liquid gallium and the N_2 cover gas in the upper plenum (Fig. 4). The prism layer meshing generates parallel prismatic layers in the liquid boundary layers adjacent to the solid boundaries with an exponential stretching factor of 1.2. The polyhedral meshing model generates the mesh within the walls of the upper plenum and the instrumentation probes (Fig. 3). The prism layers help to accurately calculate the inner surface temperature of the stainless-steel wall and the rate of heat transfer between the wall and the liquid gallium in the upper plenum. The results help select the best mesh refinement to use in the present CFD analyses based on the simulation results and the computation cost.

The sensitivity analysis examines four numerical mesh grid refinements of increasing the total count and decreasing the sizes of the mesh grid cells in the liquid gallium and in the prism layers at the solid surfaces (Table 1), namely: Coarse, Medium, Fine, and Finer mesh grids. They progressively decrease the size of the liquid base numerical cell element from 2 mm to 0.5 mm and increase the number of prism layers at the liquid solid interfaces from 4 to 12. Comparable refinements are performed of the numerical mesh grid in the stainless-steel plenum wall and the N_2 cover gas (Table 1). The total number of numerical mesh cells in the liquid upper plenum in the PLOP experiments increases from 9.16 million cells for the Coarse grid to up to 116.53 million cells for the Finer grid (Fig. 4, 5 and Table 1).

Table 1. Parameters of the numerical mesh grid refinements investigated in the of the CFD analyses of the upper plenum in the PLOP experiments.

Mesh Grid	Domain	Base Cell Size (mm)	No Prism Layers	Layer Total Thickness (mm)	Cell Count (Millions)	Total Cell Count (Millions)
Coarse	Liquid Gallium	2	4	1	5.44	9.16
	Plenum Wall	4	2	1.5	3.38	
	N_2 Cover Gas	4	2	1.5	0.33	
Medium	Liquid Gallium	1.2	6	1	11.52	16.09
	Plenum Wall	3.3	3	1.5	4.16	
	N_2 Cover Gas	3.3	3	1.5	0.4	
Fine	Liquid Gallium	1	8	1	18.39	24.47
	Plenum Wall	3	3	1.5	5.55	
	N_2 Cover Gas	3	3	1.5	0.53	
Finer	Liquid Gallium	0.5	12	1	97.89	116.53
	Plenum Wall	1	4	1.5	16.78	
	N_2 Cover Gas	1	4	1.5	1.86	

3.3.1 Sensitivity Analysis for URANS turbulence model

The performed sensitivity analyses of the effect of the numerical mesh refinements on the liquid flow and mixing in the upper plenum are for isothermal condition (T_o = 373.15 K). They use different solution convergence criteria for the SST k-ω URANS and LES turbulence models. The Grid Convergence Index (GCI) defined by Roache [1994] quantifies the solution convergence for the analyses with the URANS turbulence model. The GCI quantifies the effect of the numerical mesh grid refinement on the solution

convergence for the calculated inlet pressure, the average discharge flow velocity, and the molten gallium mass flow rate.

The GCI index utilizes a relative error of the calculated parameter of interest, n, to quantify the effect on the computation time (Table 2), formulated as:

$$GCI_n = \frac{3*|\varepsilon|}{(r_n{}^{\rho}-1)} \quad (1)$$

In this expression, the order of the utilized numerical method, $\rho = 2$ for all cases examined. The refinement ratio r_n for mesh cell "n" relative to the reference mesh cell "n-1" is calculated for the total number of the mesh cells, N, as:

$$r_n = \left(\frac{N_{n-1}}{N_n}\right)^{\frac{1}{3}} \quad (2)$$

Increasing the mesh grid refinement decreases the numerical uncertainties of the results, and hence the GCI value in Table 2. The values with the medium grid are much higher than those for both the Fine and Finer grid refinements. The obtained CFD results using the URANS turbulence model and the medium mesh grid decreases the GCI below 0.00866, however, the computational cost for the solution convergence increases rapidly with increasing the mesh refinement (Table 2). With the Fine mesh grid refinement, the solution convergence requires 11 times the CPU days for the analysis with the Coarse mesh refinement.

Table 2. Effect of mesh grid refinement on the calculated GCI in the CFD analyses of the PLOP experiments using the SST k-ω URANS turbulence model.

Mesh Grid type	Total Cell Count (millions)	Relative Refinement Ratio	URANS Turbulence Model	
			Avg. GCI	Computational Time (CPU Days)
Coarse	9.2	1	-	131.4 (1)
Medium	16.1	1.21	0.00866	230.8 (1.756)
Fine	24.4	1.39	0.00176	297.0 (2.26)
Finer	116.5	2.33	0.00019	1,449.9 (11)

3.3.2 Sensitivity Analysis for the LES turbulence model

The present CFD analyses also investigated the effect of the numerical mesh grid refinement on the solution convergence using the LES turbulence model. They compare the resolved fraction of the turbulent kinetic energy, k, for the liquid gallium in the upper plenum. The LES model calculates the velocity field using a filtered or resolved component and a residual component. The resolved component quantifies the effect of the turbulence with length scales greater than the implemented mesh grid size and the residual component uses the subgrid scale model to quantify the effect of the turbulence with smaller length scales. The calculated resolved fraction of the total turbulent kinetic energy using the subgrid scale model, R, is expressed in terms of the resolved turbulent kinetic energy, k_{res}, and the calculated turbulent kinetic energy, k_{sgs}, as:

$$R = \frac{k_{sgs}}{k_{res}+k_{sgs}} \quad (3)$$

In this expression, the sum ($k_{res} + k_{sgs}$) is the total turbulent kinetic energy. When the ratio $R = (k_{res}/k_{sgs})$ approaches unity, the turbulent kinetic energy in the solution is mostly calculated by the subgrid scale model and the LES turbulence model behaves more like a RANS model, where turbulence is primarily

modeled rather than resolved. When R approaches zero, the turbulent kinetic energy is mostly resolved, and the LES turbulence model behaves more like a Direct Numerical Simulation (DNS) model. Therefore, in the analysis with the LES turbulence model, the numerical mesh grids should be sufficiently refined so that R ≤ ~0.2 [Pope 2000].

The calculated values of k_{res} and k_{sgs} using the Medium, Fine, and Finer numerical grid refinements are compared in Table 3 for the simulations of the isothermal flow mixing in the upper plenum using the LES model. This is for liquid gallium temperature of 373.15 K and inlet flow rate of 2.246 kg/s. For all numerical mesh grid refinements investigated, $k_{res} > k_{sgs}$. The ratio k_{res}/k_{sgs} of 1.509 for the analyses with the medium mesh grid increases to 1.654 and 3.397 in the analyses with the Fine and the Finer mesh grids (Table 3).

Table 3. Mesh grid refinement effect on resolved turbulent kinetic energy with the LES model.

Mesh Grid	Total Cell Count (millions)	Relative Refinement Ratio	LES Turbulence Model		
			k_{res}/k_{sgs}	R	Computational Time (CPU Days)
Medium	16.1	1.21	1.509	0.399	331.8
Fine	24.4	1.39	1.654	0.377	453.7
Finer	116.5	2.33	3.397	0.227	1719.9

Conversely, the results in Table 3 show the value of R decreases by increasing the mesh grid refinement, from 0.399 to 0.377 and 0.227 for the Medium, Fine and Finer grids, respectively. The value of R in the analyses using the Finer mesh grid is close to the recommended value of ~0.2 for CFD simulations using the LES turbulence model [Pope 2020]. Increasing the numerical mesh grid refinement (Tables 1 and 3) markedly increases the computational time for solution convergence. The present CFD simulation with the Fine mesh grid requires 37% more computational time than with the medium mesh grid. The performed CFD analyses with the Finer mesh grid require 279% more computational time than with the Fine mesh grid.

3.4. Comparison of Calculated flow mixing using URANS and LES turbulence models

The results of the performed CFD analyses using the Fine grid refinement of the flow mixing and stratification of liquid gallium in the upper plenum in the PLOP experiments using the SST k-ω URANS and LES turbulence models and presented and discussed. These results are for an isothermal liquid gallium temperature of 373.15 K and inlet flow rate of 2.246 kg/s in the upper plenum. The analyses are carried out for a minimum of 60 s of transient simulation time, which was sufficient for the solution residuals to converge. The presented velocity contours in Fig. 6 of the liquid gallium in the upper plenum are for a plane section through the center of the two horizontal outlet legs (Section A-A in Figs. 3a and c).

The results show that the mixed flow following the inlet contraction forms a wake as it moves past the inlet thermocouple (Figs. 3a-b), affecting the shape of the inlet liquid jet (Figs. 6a-b). The results of the present CFD analysis using the URANS turbulence model show the inlet liquid jet stagnates at the bottom of the UIS tube where the exiting liquid gallium flows radially towards the plenum wall and turns upward (Fig. 6a). These results are like those of the CFD simulations reported by Hu et al. [2013] for the full scale ABTR upper plenum using the same SST k-ω turbulence model. The upward flow of the liquid gallium entering the upper plenum creates large recirculation eddies in the lower section of the plenum before exiting through the two horizontal side discharge legs (Fig. 6a). The moving liquid flow along the immersed DTS fiber tube in the upper plenum develops small local disturbances in the flow mixing patterns (Figs. 6a and b).

The performed CFD analyses of the isothermal flow experiment using the LES turbulence model predict very different and more intense flow mixing in the upper plenum than using the simpler URANS turbulence model (Figs. 6a and b). The results with the LES model show that at the high inlet flow rate into the upper plenum, the liquid jet into the plenum causes flow oscillations and breaks up into numerous small mixing eddies (Fig. 6b). These eddies intensify mixing in the lower section of the plenum above the bottom of the UIS tube and below the side discharge outlets. The analyses using the LES model indicate that the inlet flow of the liquid gallium into the upper plenum turns upward almost immediately (Fig. 6b), as opposed to those using the URANS turbulence model in which shows that the inlet flow reaches the plenum wall before turning upward (Fig. 6a). The mixing of liquid gallium in the upper section of the plenum above the side discharge legs is more intense than in the lower section of the plenum section below the discharge legs and increases with increasing the inlet mass flow rate. These results show that the URANS turbulence models cannot resolve the intense chaotic mixing in the upper plenum. Thus, despite its greater computational cost, using the LES turbulence model is the better option for simulating the complex mixing patterns within the GaTE experiment upper plenum and this model is used for the transient simulations of the PLOP experiments.

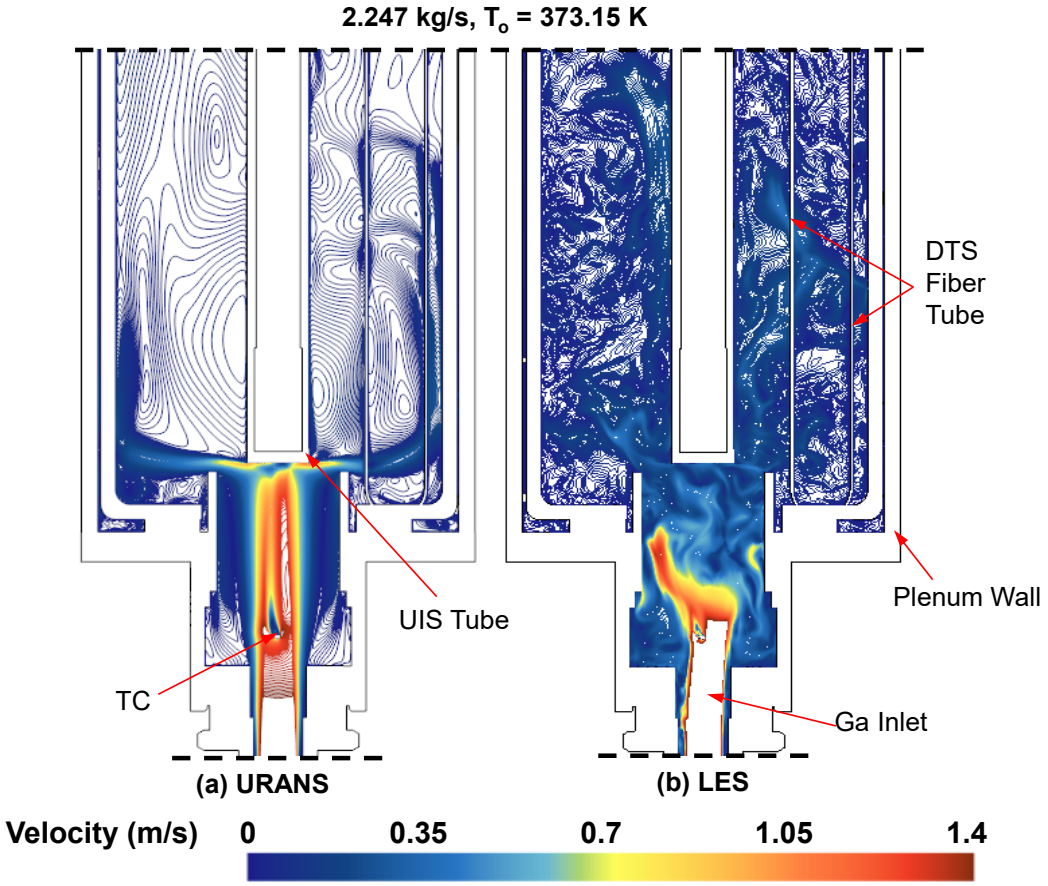

Fig. 6. Enlarged view of calculated flow velocity contours along the elevation plane B-B in Fig. 3 in the lower section of the upper plenum in the analyses with the SST k-ω URANS and LES turbulence models and a rigid free surface for isothermal condition of 373.15 K and 2.246 kg/s gallium inlet flow rate.

4.0 Numerical Simulation of the PLOP Experiments

The results presented in this section are of the performed CFD analyses using the STAR-CCM+ commercial code and the LES turbulence model to simulate liquid gallium mixing and stratification in the

upper plenum in the transient PLOP60 and PLOP40 experiments [Ward, Clark, and Bindra 2019; Bindra and Matulis 2025]. The analyses examine the effect on the results of treating the liquid gallium free surface in the upper plenum as a rigid and a non-rigid boundary. The calculated local gallium temperatures in the upper plenum of the reported PLOP60 and PLOP40 experiments are compared to the reported measurements in Figs. 7 and 8. These measurements were recorded by the DTS fiber sensor tube and the inlet thermocouple (Figs. 2, 3).

Prior to the start of the simulated transients in the experiments, the liquid gallium in the plenum is initially at the same 373.23 K temperature as that of liquid gallium entering the plenum at flow rates of 0.524 kg/s in the PLOP40 experiment and 0.786 kg/s in the PLOP60 experiment. The analyses are conducted first of the isothermal liquid gallium inlet flow at 373.15 K to establish the conditions in the upper plenum before simulating the PLOP transient. In the transient experiments, the temperature of the liquid gallium entering the plenum decreases by 50 K, from an initial value of 373.15 K to 323.15 K over a period of 17 s and remains steady thereafter [Ward, Sieh, and Bindra 2019]. The corresponding average axial velocity of the liquid gallium entering in the cylindrical pipe below the central UIS tube in the GaTE upper plenum is 40 mm/s and 60 mm/s in the PLOP40 and the PLOP60 experiment, respectively (Fig. 3). In addition to the inlet flow rate of the cooler gallium into the plenum the input to the present CFD analysis includes the reported liquid inlet temperature versus time in the experiment.

4.1. Comparisons of calculated and measured liquid temperatures in upper plenum

Figures 7a-c and 8a-c compare the calculated axial distributions of the local temperatures of liquid gallium in the upper plenum to the reported measured values along the length of the middle DTS fiberoptic probe (at r = 35.56 mm) at transient times, t = 10s, 60s, and 80 s in the experiments. The temperature measurements in these figures are of two data sets labeled T705 and T706 recorded by two different fiberoptic tubes within the steel DTS probe sheath. At t = 10s in the PLOP60 experiment with 0.786 kg/s inlet flow rate of the cooler liquid gallium, the calculated temperatures in the lower section of the plenum, extending 80 mm from the bottom of the plenum, are in good agreement with the reported measurements (Fig. 7a). In this section of the plenum, the calculated temperatures with a non-rigid gallium free surface are lower than the reported measurements early in the experiments. The difference gradually decreases with time in the experiment, and the calculated temperatures become close to the measurements (Figs. 8b and c).

The simulation results for the PLOP40 experiment with a smaller 0.524 kg/s inlet flow rate of the cooler liquid gallium show a similar trend to those for the PLOP60 experiment. At time t = 10 s, the calculated temperatures are within the range of the reported temperature measurements in the upper plenum (Figs. 7a and 8a). At transient times t = 60 s and 80 s, the calculated temperatures are in good agreement with the reported measurements at the axial locations below Z = 125 mm, but higher than measured values in the plenum immediately below the side discharge legs (Z = 125-250 mm (Figs. 8b and c).

The calculated temperatures of liquid gallium close to the free surface in the upper plenum of the PLOP60 and PLOP40 experiments are slightly higher than the reported measurements (Figs. 7 and 8). For the PLOP60 and PLOP40 experiments, the results of the analyses with a rigid and a non-rigid free surface show a slight effect on the calculated liquid temperature in the top section of the plenum. At the inlet flow rate of 0.786 kg/s in the PLOP60 experiment, the calculated results show a small difference between the calculated and reported temperatures (< ~4 K) in the top section of the plenum with a rigid or a non-rigid liquid free surface (Figs. 7a-c). In the PLOP40 experiment at an inlet liquid flow rate of 0.524 kg/s, the calculated liquid temperatures in the analyses with a rigid and a non-rigid free surface (Figs. 8a-c) are close to the reported measurements in the top section of the plenum to within < ~5 K. The results with a rigid surface show somewhat large fluctuations caused by the reflection of the flow from the liquid surface. In the analysis with a non-ridge liquid free surface results show formation of a larger number of

small liquid mixing eddies in the upper section of the plenum, producing smaller fluctuations in the local temperature

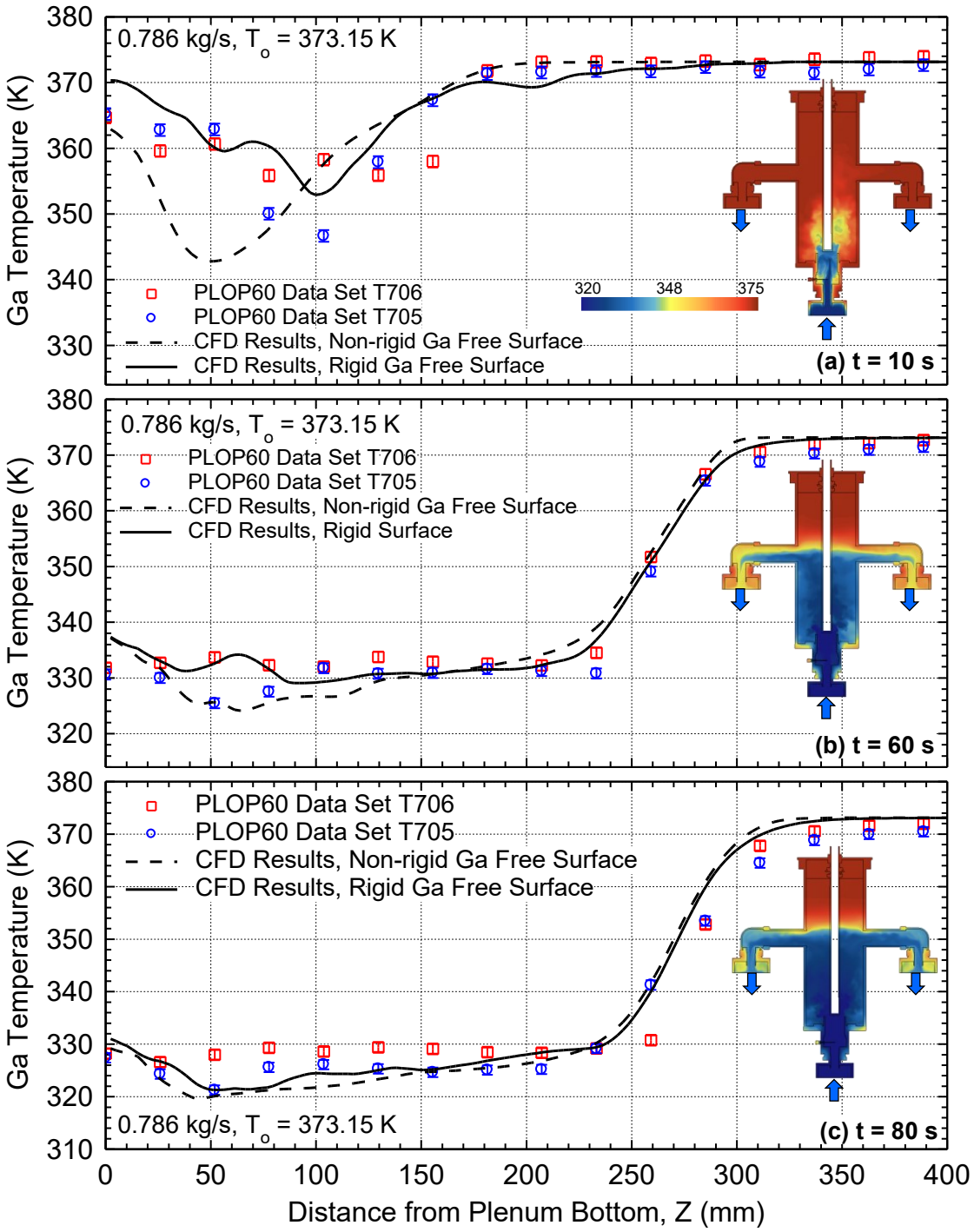

Fig. 7. Comparison of calculated and measured axial profiles of the local liquid gallium temperature in the upper plenum along the middle DTS fiber probe in PLOP60 experiment [Ward, Clark, and Bindra 2019].

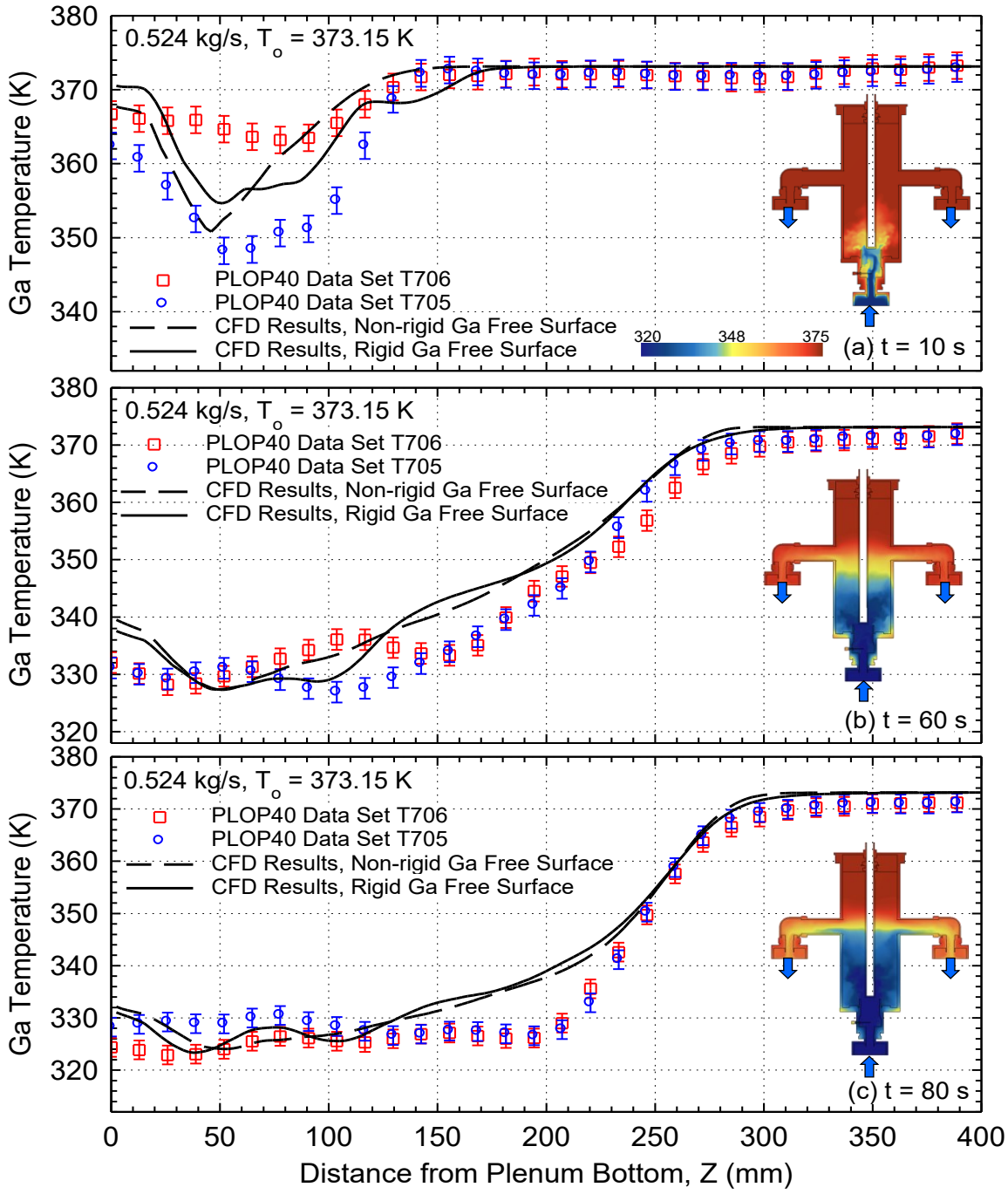

Fig. 8. Comparison of calculated and measured axial profiles of the local liquid gallium temperature in the upper plenum along the middle DTS fiber probe in PLOP40 experiment [Ward, Clark, and Bindra 2019].

Figures 9 and 10 show three-dimensional field plots of the calculated local gallium temperature at axial locations along the three vertical segments of the DTS fiber probe tube (at r = 11.8, 35.6, 56.9 mm) in the transient PLOP40 experiment. The temperature fields in Figs. 9a, c, and e and Figs. 9b, d, and f are those calculated in the present analysis with a rigid and a non-rigid liquid free surface, respectively. The area between horizontal lines in these plots indicates the axial location of the side discharge legs (Fig. 3). At t

< 10 s the analysis with a rigid free surface shows greater mixing at the lower section of the plenum along the innermost DTS probe segment (r = 11.8 mm) (Figs. 9a and b), compared to that with a non-rigid free surface. As the transient continues the liquid temperature in the plenum section below the discharge legs decreases with increased inlet flow of the colder gallium. In the top section of the plenum the liquid temperature within the thermally stratified liquid layer remains close to the initial temperature, T_o (Figs. 8 and 9).

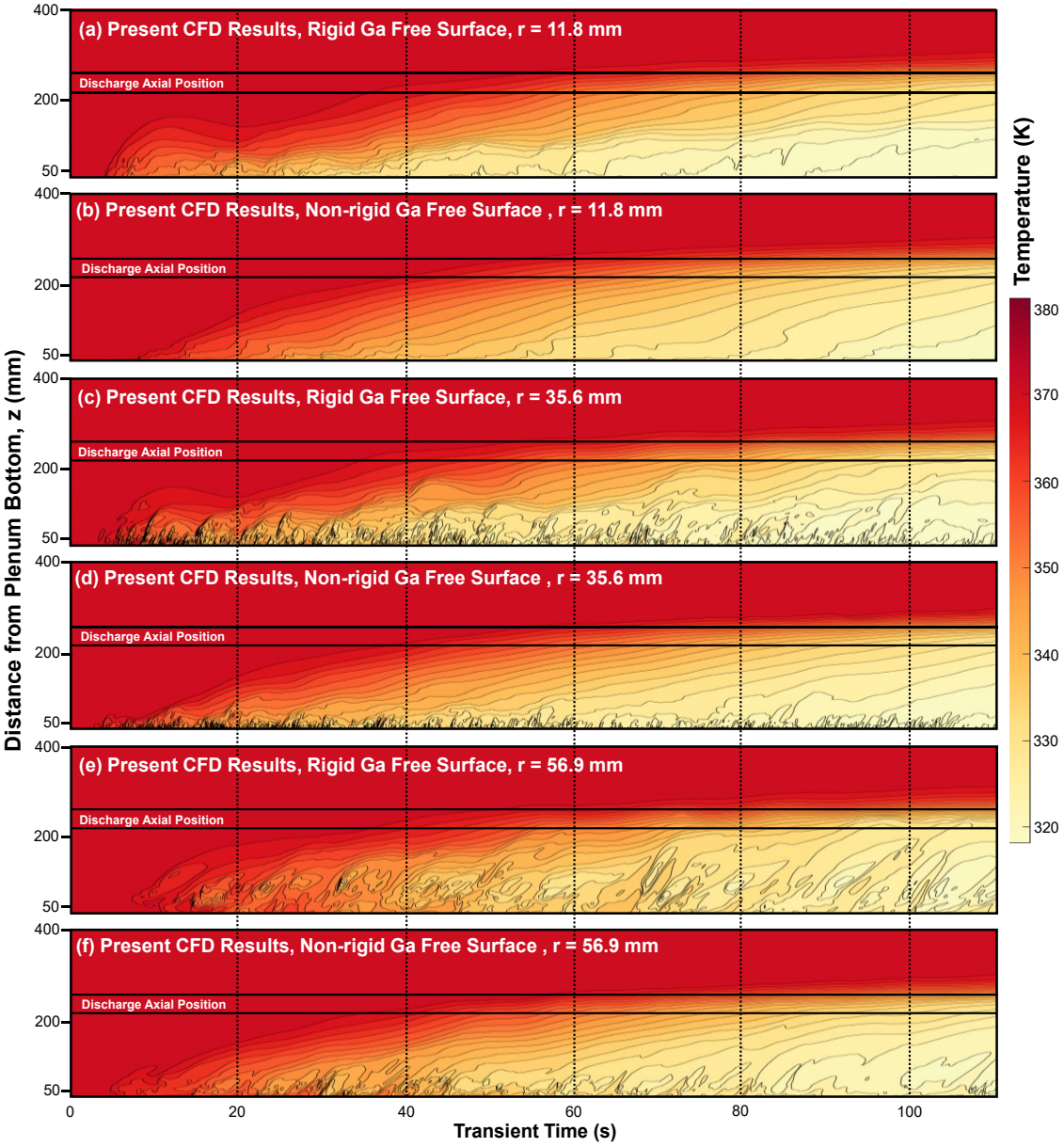

Fig. 9. Images of the calculated temperatures contours in the plenum at the DTS probe radial locations (r = 11.8, 35.6, 56.9 mm) in the present analysis with a rigid and a non-rigid gallium free surface of the PLOP40 experiment.

At the locations of the middle and outermost DTS radial locations (r = 35.6 mm and 56.9 mm) the analysis with a rigid gallium free surface (Figs. 9c and e) shows more intense liquid mixing and temperature fluctuations in the lower section of the plenum, compared to the analysis with a non-rigid

free surface (Figs. 9d and f). Thus, even though the calculated temperatures in the analysis with a rigid and a non-rigid liquid free surface in the plenum are close (Figs. 8a-c) the fluctuations of the liquid free surface in latter affect the flow mixing in the upper but not in lower section of the plenum.

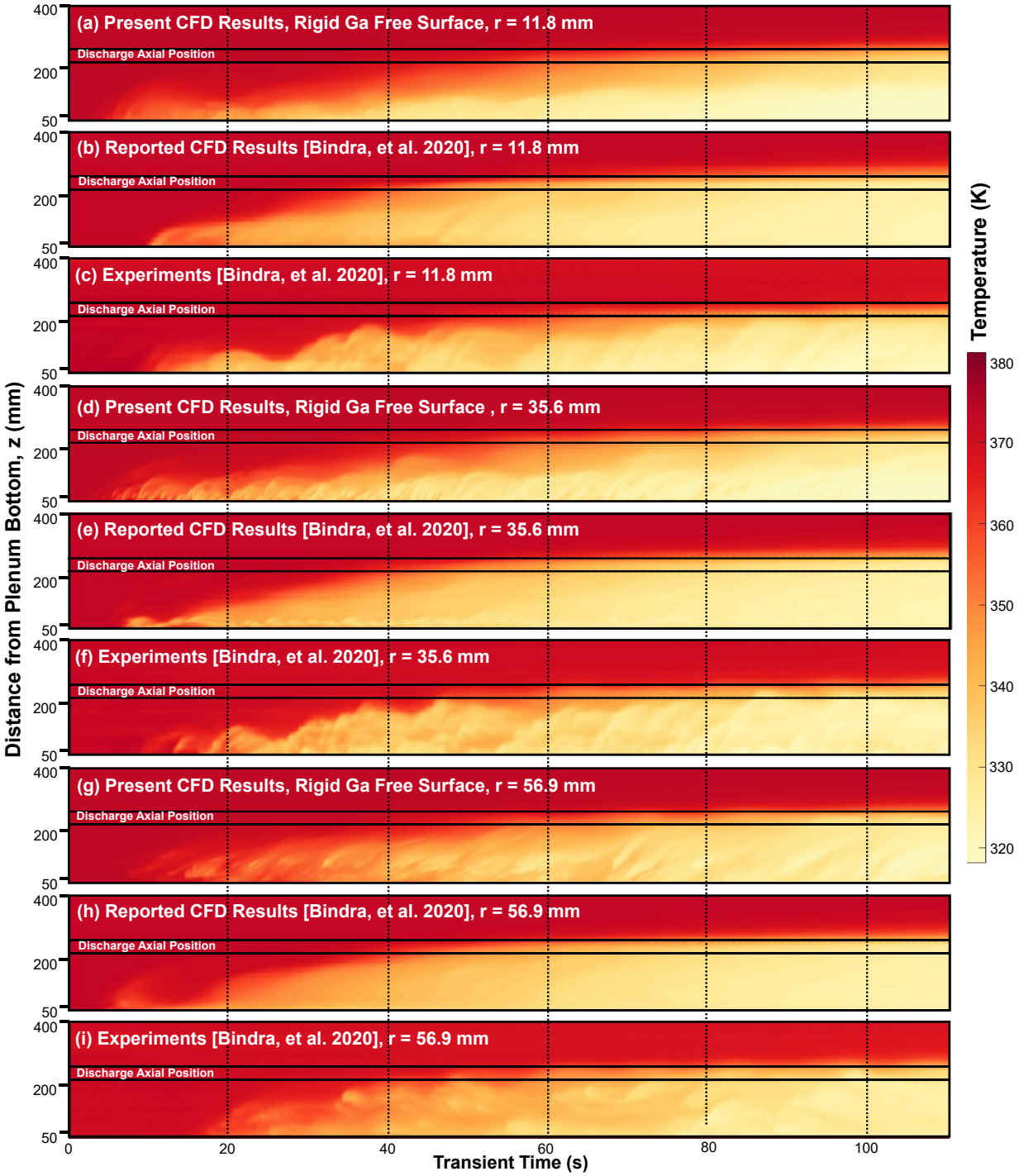

Fig. 10. Comparison of calculated temperature contours at radial locations of the DTS probe (r = 11.8, 35.6, 56.9 mm) in present analysis with a rigid free surface to those obtained in the analysis by Bindra et al. [Bindra, et al. 2020] using the CFX CFD code, also assuming a rigid free surface, and the reported experimental measurements in the PLOP40 experiment.

Figure 10 compares the obtained images of the temperature field in the present CFD analysis to those of Bindra et al. [2020] using the CFX CFD code. Both results are for a rigid gallium free surface in the plenum of the PLOP40 experiment [Ward, Clark, and Bindra 2019; Bindra, et al. 2020] and at axial locations along the three vertical segments of the DTS fiber tube (at r = 11.8, 35.6, 56.9 mm). The results of the present CFD analysis using the STAR-CCM+ commercial code (Figs. 10a, d, and g) show larger temperature fluctuations and the formation of more mixing eddies than the reported CFX CFD simulations of Bindra et al. [2020] (Figs. 10b, e, and h). These fluctuations are in closer agreement with those in the reported measurements for the PLOP40 experiments (Figs. 10c, f, and i). Both the present results and reported CFD results of Bindra et al. [2020] use the LES turbulence model with WALE subgrid scale model and are for a rigid liquid free surface. The present analysis uses a refined mesh grid of 18.39 million mesh elements in the plenum (Table 1) vs 2.426 million mesh elements in reported analysis [ref 14,28], which may explain the differences in the results.

The present analysis (Figs. 10a, d, and g) also predicts that the liquid mixing front in the plenum reaches the height of the side discharge later in time than the reported CFD results of Bindra et al. [ref 28] (Figs. 10b, e, and h) (t = ~59 vs ~49 s for r = 11.8 mm, t = ~58 vs ~46 s for r = 35.6 mm, and t = ~56 vs 45 s for r = 56.9 mm). These predicted times in the present simulations are in good agreement with the reported experimental measurements for the middle (t = ~59 s for r = 35.6 mm) and the outer (t = ~57 s for r = 56.9 mm) DTS segments. Both CFD analyses (Figs. 10a and b) predict that the liquid mixing front reaches the height of the side discharge tubes for the innermost probe location earlier than reported in the PLOP40 experiment (t = ~64 s for r = 11.8 mm) (Fig. 10c).

In summary, the results of the present CFD analyses of the transients in the PLOP60 and PLOP40 experiments demonstrate that accounting for a non-rigid liquid free surface in the plenum is more realistic as it affects the liquid mixing the upper section of the plenum (Fig. 9). The analyses results show larger differences between the calculated temperatures below the liquid free surface with a rigid or a non-rigid liquid free surface (Figs. 7, 8).

4.2. Comparisons of calculated and measured averaged axial velocities in upper plenum

Figures 11 and 12 compare the calculated and the reported measurements of the time averaged axial velocity of liquid gallium at different axial and radial positions in the plenum of the PLOP60 and PLOP40 experiments, respectively [Ward, Sieh, and Bindra 2019]. The reported measurements are for an isothermal temperature of 373.15 K and liquid gallium inlet flow rates of 0.786 kg/s (PLOP60) and 0.524 kg/s (PLOP40) into the upper plenum. The measured axial velocity profiles by the UDV probes, mounted in the plenum at radial positions of r = 36, 47, and 58 mm (Fig. 3) are those of the averaged values in four separate 9.5 s periods (labeled Data Sets 1-4) [Ward, Sieh, and Bindra 2019]. The reported values of these time-average axial velocities, based on the measurements of the UDV probes mounted at the three radial locations in the plenum, show considerable variations (Figs 11a-c and 12a-c). This may be attributed to the intense turbulent mixing of liquid gallium in the upper plenum, demonstrated by the results of the performed CFD analyses (Figs. 6). The sign of the flow average velocity indicates the liquid gallium flow direction within the plenum. The results in the PLOP40 and PLOP60 experiments show similar trends in the recorded flow direction at the three radial locations of the UDV probe (Figs. 11 and 12). The flow direction indicated by the innermost UDV probe (r = 36 mm) is upward (with a positive velocity) (Figs. 11a and 12a), and downward (with a negative velocity) for the outermost UDV probe (r = 58 mm) (Figs. 11c and 12c). The axial flow directions indicated by the measurements of the middle UDV probe at r = 47 mm in the plenum varies between upward and downward (Figs. 11b and 12b).

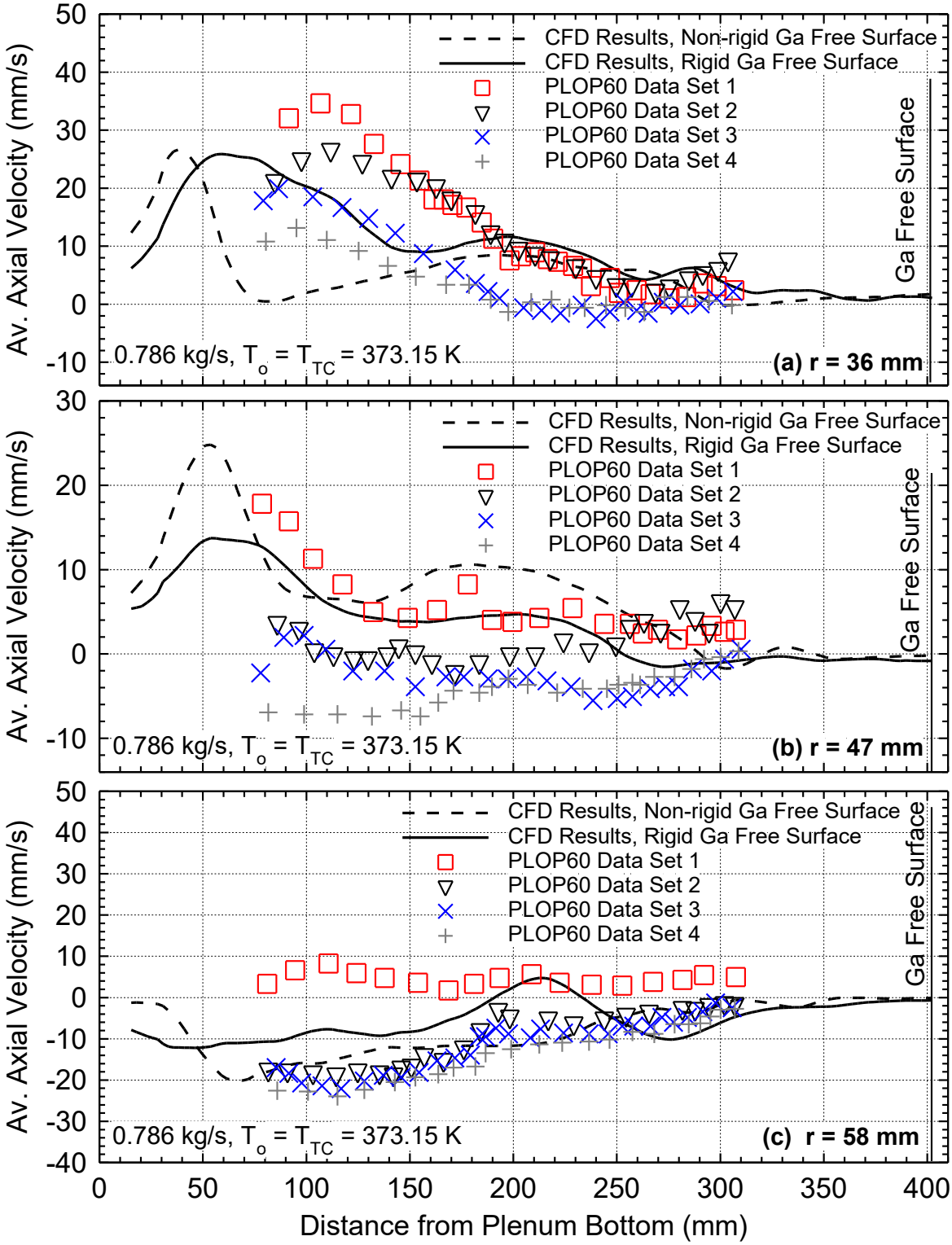

Fig. 11. Comparison of the axial profiles of the calculated and the measured time-averaged velocity in the upper plenum of the PLOP60 experiment using the UDV probe [Ward, Sieh, and Bindra 2019].

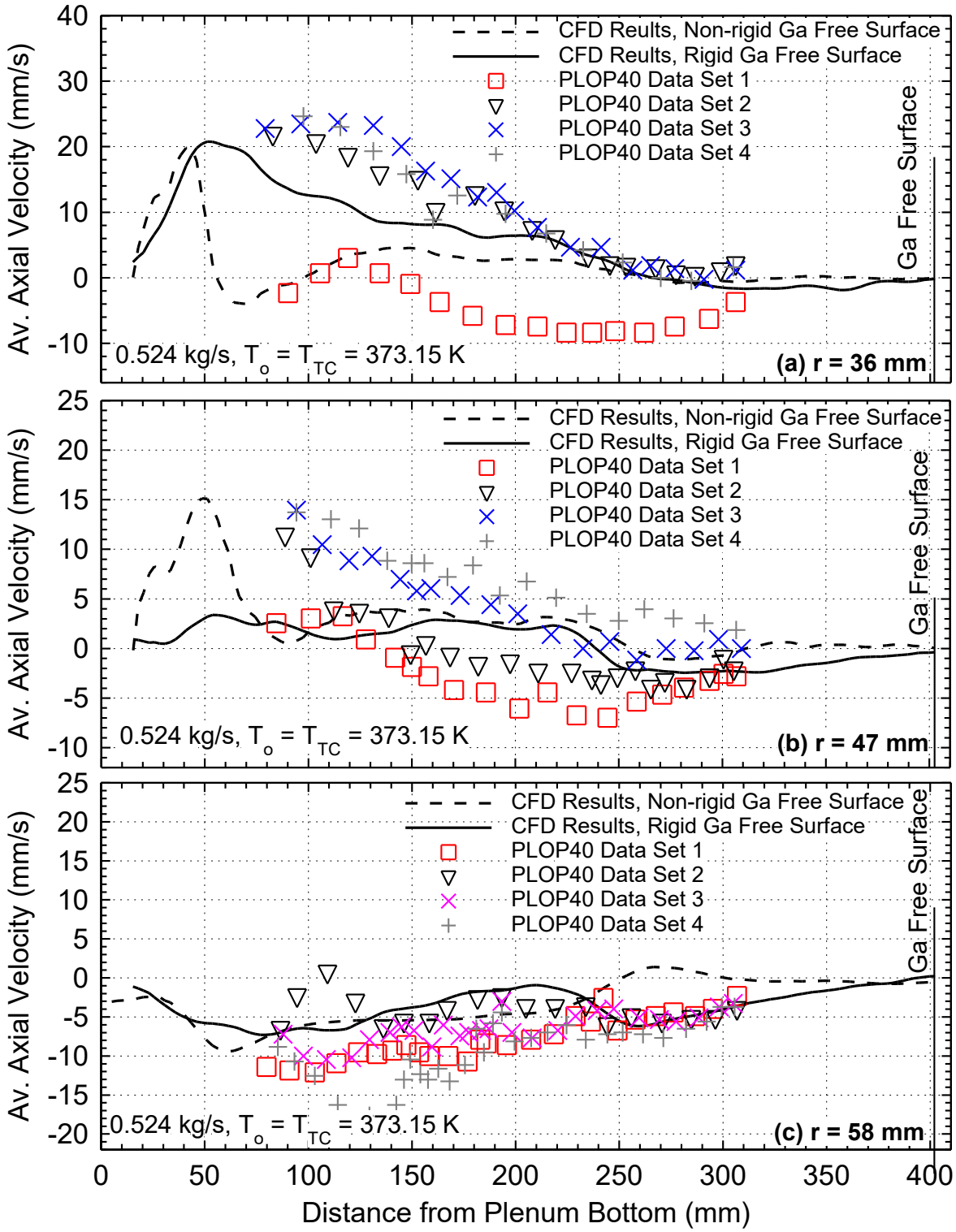

Fig. 12. Comparison of the axial profiles of the calculated and the measured time-averaged velocities in the upper plenum of the PLOP40 experiment using the UDV probe [Ward, Sieh, and Bindra 2019].

Figure 11 compares the calculated liquid axial velocities in the plenum, averaged over a period of 30 s of simulation time, to the reported measurements in the isothermal PLOP60 experiment with liquid gallium inlet flow rate of 0.786 kg/s at 373.15 K. Fig. 12 compares the calculated results to the reported measurements for the PLOP40 experiment performed at liquid gallium inlet flow rate of 0.524 kg/s and 373.15 K. The calculated values are of the present CFD analyses with a rigid and a non-rigid gallium free surface in the plenum. The calculated velocity values are consistent with the reported experimental measurements, both approaching zero close to the gallium free surface at Z = 403 mm in the plenum. The axial profiles of the calculated average velocities in the plenum for the PLOP60 and PLOP40 experiments fall within those reported in four experimental data sets. These velocities are positive (pointing upward) as indicated by the UDV probe located in the plenum at r = 36 mm, while those indicated by the probe at r = 58 mm are negative (pointing downward) (Figs. 11a,c and 12a,c). These results indicate the induced turbulence and mixing of the liquid gallium in the plenum of the PLOP experiments. They also show that the calculated axial velocities in the plenum of the PLOP60 and PLOP40 experiments in the present analyses with the LES turbulence model, and the Fine numerical mesh grid are generally in good agreement with reported experimental data (Figs. 11a-c and 12a-c).

5.0 Summary and Future Work

This work details the performed CFD analyses at the UNM-ISNPS and during the second year of the 2023 DOE NUEP IRP award entitled: *Exascale Simulation of Thermal-Hydraulics Phenomena in Advanced Reactors and Validation Using High Resolution Experimental Data*. The aim is to build expertise and demonstrate capabilities for large scale CFD modeling and simulation of thermal-hydraulic phenomena in advanced reactors at UNM and CCNY. The performed CFD analyses at the UNM-ISNPS are of the conducted Protected Loss of Power transients in the experiments carried out in the GaTE facility at Purdue University using liquid gallium simulant. The obtained CFD analyses results of liquid mixing and stratification below the free surface in the plenum of the reported experiments are benchmarked against the measurements for the PLOP60 and PLOP40 experiments carried out at Purdue University.

The performed CFD analyses using the lower cost URANS SST k-ω turbulence model with a Fine mesh grid could not capture the complex mixing patterns occurring in the plenum, which are resolved in subsequent analyses using the LES turbulence model, instead. In the performed analyses using the LES turbulence model and Fine and the Finer mesh grids the calculated fractions of the total turbulent kinetic energy of 0.227 and 0.377 are close to the recommended value of 0.2 for solution convergence. Since the results of the analyses using both mesh grids are close, despite the much higher computation cost of that using the Finer grid, the present CFD analyses used Fine mesh grid and the LES turbulence model. The analyses results show intense turbulent mixing of liquid gallium in the upper plenum and in the vicinity of the inlet flow nozzle to the plenum.

The present CFD analyses investigated the effects of considering a rigid and a non-rigid liquid free surface on the induced liquid mixing and stratification as well as on the calculated temperatures and velocity fields in the plenum. The liquid average temperature in the lower section of the plenum decreases rapidly with time due to the liquid intense turbulent mixing. Less intense liquid mixing occurs in the top section of the plenum above the side outlet legs, where a stratified layer of hot gallium forms below the liquid free surface. The extent of this layer decreases with increased injection velocity of cooler Ga into the plenum.

In the analysis with a non-rigid free surface, the liquid temperature below the free surface decreases sooner below the initial value of 373.15 K than in the analysis with a rigid free surface. However, the differences between the calculated liquid temperatures in the plenum in the analysis with a rigid and a non-rigid liquid free surface are small for flow rates of 0.524 and 0.786 kg/s in the PLOP40 and PLOP60

experiments, respectively. The axial profile of the liquid temperatures in the plenum for the analysis with a rigid and a non-rigid liquid free surface are close in the lower section of the plenum below the side discharge legs. The formation of a greater number of small turbulent eddies in the top section of the plenum and near the free surface in the present simulations with a non-rigid free surface, slightly decreases the thickness of the stratified liquid region.

The calculated temperatures of the liquid gallium near free surface for the simulated transients in the PLOP60 and PLOP40 experiments are in good agreement with the reported measurements. The calculated temperatures are slightly higher than the reported measurements in the top section of the plenum with either a rigid or a non-rigid liquid free surface. The calculated values for the PLOP60 experiment with liquid Ga inlet flow rate of 0.786 kg/s agree with the reported experimental measurements to within < ~4 K. The calculated liquid temperatures in the PLOP40 experiment with liquid Ga inlet flow rate of 0.524 kg/s agree with reported measurements in the top section of the plenum to within < ~5 K. The calculated values and axial profiles of the time-average liquid velocities at different radial locations in the plenum fall mostly within the range of the reported experimental measurements.

The results of the present CFD simulations using the STAR-CCM+ code are overall in good agreement with those reported for the liquid gallium PLOP experiments conducted at Purdue University. The results indicate that simulating the liquid gallium free surface can affect the calculated liquid mixing in the plenum as well as the extent and oscillations of the hot liquid stratified layer below the liquid free surface in the plenum. These oscillations could cause thermal stress in the structures within the pool and in the top section of the reactor core. Planned future work for the third year of the IRP DOE NEUP award will simulate the helium-air gas mixing experiments performed at CCNY. ***However, we plan to request a 6-month no-cost extension of the present award to make up for the delay in starting the CCNY subaward to UNM at the start of the project.***

Acknowledgements

We wish to thank Professor Hitesh Bindra and John Matulis at Purdue University for graciously providing the experimental data and the solid geometry CAD files used in this work. We are also grateful for the access to the resources of the High-Performance Computing Center at Idaho National Laboratory, which is supported by the Office of Nuclear Energy of the U.S. Department of Energy and the Nuclear Science User Facilities under Contract No. DE-AC07-05ID14517 and the University of New Mexico's Center for Advanced Research Computing, supported in part by the National Science Foundation, for providing access to its high-performance computing capabilities.

This research is supported by a Department of Energy Nuclear Engineering University Program Integrated Research Project grant DE-NE0009420 through a subaward from the City College of New York to the University of New Mexico CM00011961-00.

References

M. J. ASSAEL, et al., "Reference data for the density and viscosity of liquid cadmium, cobalt, gallium, indium, mercury, silicon, thallium, and zinc." Journal of Physical and Chemical Reference Data, **41**, *3*, 033101 (2012); https://doi.org/10.1063/1.4729873

H. BINDRA AND J. MATULIS, Purdue University, GaTE protected loss of power experimental temperature measurements, Personal Communication (2025).

H. BINDRA, B. WARD, R.-u. S. NAMALA, T. SUMNER, "Computational-Experimental Study to Simulate Mixing and Thermal Stratification in SFRs," NEUP Project 16-10579 – FINAL REPORT, Purdue University, West Lafyette, IN, USA (2020).

Y. I. CHANG, P. J. FINCK, C. GRANDY, "Advanced burner test reactor preconceptual design report," ANL-ABR-1, Argonne National Laboratory, Argonne, IL (2008).

R. HU, et al., "Development of SFR Primary System Simulation Capability for Advanced System Codes," Argonne National Laboratory technical report ANL/NE-13/11, Argonne, IL, USA (2013).

INTERNATIONAL ATOMIC ENERGY AGENCY, 2013, "Design Features and Operating Experience of Experimental Fast Reactors," IAEA Nuclear Energy Series, NP-T-1.9, Vienna, Austria (2013).

J. LAROCQUE, "Heat Transfer Simulation in Swirling Impinging Jet," Institut National Polytechnique de Grenoble, Division of Heat Transfer, Grenoble, France (2004).

B. E. LAUNDER AND D. B. SPALDING, "The Numerical Computation of Turbulent Flows," Computational Methods Appl. Mech. Engr., **3**, 269 – 289 (1974).

E. W. LEMMON, I. H. BELL, M. L. HUBER, M. O. MCLINDEN, "Thermophysical Properties of Fluid Systems" in NIST Chemistry WebBook, NIST Standard Reference Database Number 69, Eds. P.J. Linstrom and W.G. Mallard, National Institute of Standards and Technology, Gaithersburg MD, https://doi.org/10.18434/T4D303, (retrieved September 2024).

H. MOCHIZUKI AND H. YAO, "Analysis of thermal stratification in the upper plenum of the "Monju" reactor." Nuclear Engineering and Design, **270**, 48–59 (2014); https://doi.org/10.1016/j.nucengdes.2013.12.049

S. OHNO, H. OHKI, A. SUGAHARA, H. OHSHIMA, "Validation of a computational simulation method for evaluating thermal stratification in the reactor vessel upper plenum of fast reactors." Journal of Nuclear Science and Technology, **48**, *2*, 205–214 (2011); https://doi.org/10.1080/18811248.2011.9711694

S. B. POPE, *Turbulent Flows*, Cambridge University Press, Cambridge, MA (2000).

P. J. ROACHE, "Perspective: A Method for Uniform Reporting of Grid Refinement Studies," Journal of Fluids Engineering, **116**, 405 (1994).

S. B. RODRIGUEZ AND M. S. EL-GENK, "Coupled Computational Fluid Dynamics and Heat Transfer Analysis of VHTR Lower Plenum". *Proc: 11th International Congress on Advances in Nuclear Power Plants (ICAPP-2011)*, Nice, France, May 2–5, 2011, Paper # 11247 2011

T. SAKAMOTO, M. SHIBAHARA, T. TAKATA, A. YAMAGUCHI, "Numerical study of three-dimensional thermal hydraulics effect on thermal stratification phenomena in upper plenum of MONJU. *Proc. Korea-Japan Symposium on Nuclear Thermal Hydraulics and Safety (NTHAS-7)*, Chuncheon, South Korea, November 14-17, 2010.

SIEMENS PLM, STAR-CCM+ version 18.06 (2023), https://plm.sw.siemens.com/en-US/simcenter/fluids-thermal-simulation/star-ccm/

J. SMAGORINSKY, "General Circulation Experiments with the Primitive Equations I. The Basic Experiment," Dept. of Commerce, Monthly Weather Report, **91**, *3*, 99 – 164 (1963).

U.S. DEPARTMENT OF ENERGY, "Sodium-Cooled Fast Reactor Fact Sheet," Department of Energy Office of Nuclear Energy (2021).

B. WARD, J. CLARK, H. BINDRA, "Thermal stratification in liquid metal pools under the influence of penetrating colder jets," Experimental Thermal and Fluid Science, **103**, 118-125 (2019); https://doi.org/10.1016/j.expthermflusci.2018.12.030

B. WARD, T. HOPKINS, H. BINDRA, "Experimental Validation of CFD Models Capturing the Thermal-Hydraulics in Liquid Metal Cooled Reactor Plena," *Proc. International Conference on*

Nuclear Engineering, American Society of Mechanical Engineers, Virtual, Online, August 4–5, 2020, ICONE2020-16661, V003T12A037.

B. WARD, B. SIEH, H. BINDRA, "Experimental measurement of liquid metal flow fields in a scaled SFR upper plenum," *Proc: 18th International Topical Meeting on Nuclear Reactor Thermal Hydraulics (NURETH-18)*, Portland, OR, August 18–23, 2019.

Z. WU, et al., "A status review on the thermal stratification modeling methods for Sodium-cooled Fast Reactors," Progress in Nuclear Energy, **125**, 103369 (2020); https://doi.org/10.1016/j.pnucene.2020.103369

B. ZAMORA, "Comparative assessment of liquid sodium and gallium as emergency coolants in nuclear energy applications." Journal of Heat Transfer, **142**, *12*, 122602 (2020); https://doi.org/10.1115/1.4048136

K. ZWIJSEN, D. DOVIZIO, V. MOREAU, F. ROELOFS, "CFD modelling of the CIRCE facility," Nuclear Engineering and Design, **353**, 110277 (2019); https://doi.org/10.1016/j.nucengdes.2019.110277